Field-Induced Antiferromagnetism in the Kondo Insulator

K. S. D. Beach* and Patrick A. Lee
Department of Physics, Massachusetts Institute of Technology, Cambridge Massachusetts 02139, USA

P. Monthoux
Cavendish Laboratory, University of Cambridge, Cambridge CB3 0HE, United Kingdom
(Received 12 June 2003; published 16 January 2004)

The Kondo lattice model, augmented by a Zeeman term, serves as a useful model of a Kondo insulator in an applied magnetic field. A variational mean field analysis of this system on a square lattice, backed up by quantum Monte Carlo calculations, reveals an interesting separation of magnetic field scales. For Zeeman energy comparable to the Kondo energy, the spin gap closes and the system develops transverse staggered magnetic order. The charge gap, however, remains robust up to a higher hybridization energy scale, at which point the canted antiferromagnetism is exponentially suppressed and the system crosses over to a nearly metallic regime. Quantum Monte Carlo simulations support this mean field scenario. An interesting rearrangement of spectral weight with magnetic field is found.

DOI: 10.1103/PhysRevLett.92.026401 PACS numbers: 71.27.+a, 71.10.Fd, 71.30.+h

The unusual properties of heavy fermion materials are the result of strong interactions between their mobile *spd* and tightly bound f electrons. In the standard picture [1], a broad conduction band is intersected by a nearly flat band of renormalized core levels. Hybridization produces a gapped band structure with extremely shallow dispersion near the band edge. Since RKKY-mediated antiferromagnetism competes with this hybridization mechanism, heavy fermion systems typically live at the edge of magnetic instability [2].

The Kondo lattice model (KLM) provides an approximate description of the heavy fermion materials. At half-filling, local singlet formation dominates whenever the Kondo coupling J exceeds some critical value J_c; RKKY antiferromagnetism wins out otherwise. The large J regime is believed to describe such Kondo insulators as $Ce_3Bi_4Pt_3$, CeRhAs, CeRhSb, YbB_{12}, and SmB_6.

An applied magnetic field interferes with the singlet-RKKY competition by favoring triplet rather than singlet formation at each site. Accordingly, it suppresses the singlet amplitude and thus has the potential to stabilize an antiferromagnetic phase, even in the $J > J_c$ region. Moreover, the Zeeman splitting lifts the degeneracy of the spin up and spin down bands, shifting them with respect to one another and potentially closing the charge gap. Indeed, transport measurements of $Ce_3Bi_4Pt_3$ in high magnetic fields [3,4] indicate that its resistivity plummets to a low impurity-dominated value at a critical field on the order of 50 T.

In this Letter, we show by variational mean field and quantum Monte Carlo (QMC) calculations that as the applied field is ramped up the Kondo insulator ground state of the KLM with Zeeman splitting (KLM + Z) gives way to a canted antiferromagnetic phase. At sufficiently large field, the localized spins become polarized and the system crosses over to a nearly metallic regime with an exponentially small charge gap. We have devised a QMC formulation that is free of the notorious fermion sign problem for all values of the applied field. Since the QMC data are exact, it provides an important confirmation of the mean field predictions. Our QMC efforts are closely related to the zero-field work of Capponi and Assaad [5]. A mean field calculation in zero field has previously been carried out by Zhang and Yu [6].

The KLM + Z describes a half-filled conduction band interacting with a lattice of localized spins $\{\hat{\mathbf{S}}_i\}$. The net magnetic moment at each site is coupled to an external field. The Hamiltonian is $\hat{H} = \hat{H}_t + \hat{H}_{JB}$, where

$$\hat{H}_t = -t\sum_{\langle ij\rangle}(c_i^\dagger c_j + c_j^\dagger c_i),$$

$$\hat{H}_{JB} = J\sum_i \frac{1}{2}c_i^\dagger \boldsymbol{\sigma} c_i \cdot \hat{\mathbf{S}}_i - B\sum_i\left(\frac{1}{2}c_i^\dagger \sigma^3 c_i + \hat{S}_i^3\right). \quad (1)$$

Here, t, J, and B are the hopping, Kondo coupling, and magnetic field, respectively. The spinor $c^\dagger = (c_\uparrow^\dagger \; c_\downarrow^\dagger)$ is the creation operator for the conduction electrons. The lattice is taken to be square, its bipartite nature being essential to our QMC scheme.

Variational mean field.—Take $\hat{\mathbf{S}} = \frac{1}{2}f^\dagger \boldsymbol{\sigma} f$, subject to the constraint $f^\dagger f = 1$, where $f^\dagger$ (f) is the creation (annihilation) operator of a fictitious, dispersionless f band. At the mean field level, it is sufficient to enforce the constraint on average and require only that $\langle f^\dagger f\rangle = 1$. In the f language, the local spin singlet operator is $f^\dagger c$.

A comprehensive variational calculation of the ground state must incorporate all of the following: hybridization between the c and f bands (singlet formation), antiferromagnetism transverse to the field, and magnetism parallel to the field. A suitable trial wave function is the ground state of the mean field Hamiltonian

 0031-9007/04/92(2)/026401(4)$22.50

$$\hat{H}_{\mathrm{MF}} = \hat{H}_t - \sum_i \left[V^* f_i^\dagger c_i + V c_i^\dagger f_i + \frac{M_f}{2}(-1)^i c_i^\dagger \sigma^1 c_i + \frac{B_f}{2} c_i^\dagger \sigma^3 c_i + \frac{M_c}{2}(-1)^{i+1} f_i^\dagger \sigma^1 f_i + \frac{B_c}{2} f_i^\dagger \sigma^3 f_i \right]. \quad (2)$$

It contains five symmetry-breaking terms, controlled by the variational parameters $\{V_m\} = \{V, M_c, M_f, B_c, B_f\}$. The variational ground state energy $\mathcal{U}[\{V_m\}]$ is the expectation value of the exact Hamiltonian evaluated in the ground state of $\hat{H}_{\mathrm{MF}}$. $\{V_m\}$ is then chosen such that $\mathcal{U}$ is minimized. Figure 1 depicts the resulting phase diagram.

The singlet regime is characterized by nonzero hybridization ($V \neq 0$) and the absence of magnetic order ($M_{c,f} = 0$, $B_{c,f} = B$). The energy levels, given by

$$E^n_{\boldsymbol{k}s} = \tfrac{1}{2}(\varepsilon_{\boldsymbol{k}} - sB + n\sqrt{\varepsilon_{\boldsymbol{k}}^2 + 4V^2}\,) \quad (3)$$

with $\varepsilon_{\boldsymbol{k}} = -2t\sum_{l=1}^{d}\cos k_l$ (for a d-hypercubic lattice), are parametrized by the band index $n = \pm$ and spin projection $s = \pm(\uparrow, \downarrow)$. In the $B = 0$ case (inset of Fig. 3 below), the band separation takes its minimum, $2V$, on the surface $|k_1| + \cdots + |k_d| = \pi$ ($\varepsilon_{\boldsymbol{k}} = 0$). The band gap, however, is indirect: promoting a quasiparticle from the top of the lower band [at $\boldsymbol{Q} = (\pi, \ldots, \pi)$] to an arbitrary momentum state in the upper band costs $\omega^{\mathrm{qp}}(\boldsymbol{k}) = E^+_{\boldsymbol{k}} - E^-_{\boldsymbol{Q}}$; around its minimum, $\omega^{\mathrm{qp}}(\boldsymbol{k}) \approx 2\Delta_{\mathrm{K}} + (1/2m^*)|\boldsymbol{k}|^2$, where $4V^2 = 2\Delta_{\mathrm{K}}(2\Delta_{\mathrm{K}} + W)$ and $W = 4dt$ is the noninteracting bandwidth. The so-called Kondo energy, $\Delta_{\mathrm{K}}(<V)$, sets the scale for both the charge gap ($\Delta_{\mathrm{c}} = 2\Delta_{\mathrm{K}}$) and the ground state energy shift ($U[V] - U[0] \approx -\Delta K$).

Now consider $B \neq 0$. Throughout the singlet phase, V is independent of the applied field. Thus, according to Eq. (3), the hybridized bands simply shift with respect to one another in response to the applied field and the charge gap decreases monotonically: $\Delta_{\mathrm{c}} = 2\Delta_{\mathrm{K}} - |B|$. Before the charge gap closes completely, however, magnetic order sets in ($|B| = B_{\mathrm{c}} \lesssim 2\Delta_{\mathrm{K}}$). The localized spins develop a uniform moment directed with the field and a staggered moment perpendicular to it. The electrons do the same but are "effectively diamagnetic," canting *against* the field. As $|B|$ increases, V begins to falls off and vanishes at $|B| = B'$. When $|B| = B'' \approx \max(J/4, B')$, $\langle \frac{1}{2} c_i^\dagger \sigma^3 c_i \rangle$ changes sign.

Naively, one might have expected the charge gap to close at $|B| = 2\Delta_{\mathrm{K}}$. As shown in Fig. 2, however, the incipient antiferromagnetism prevents the level crossing by mixing the $(c, f)_{\boldsymbol{k}\uparrow}$ and $(c, f)_{\boldsymbol{k}+\boldsymbol{Q}\downarrow}$ bands. The charge gap has the behavior shown in Fig. 1 (side set, right): it decreases linearly with $|B|$ in the singlet phase, resurges in the canted antiferromagnetic phase, and finally collapses to an exponentially small value in the nearly metallic regime ($|B| \gtrsim B'''$, where the local spins have saturated and the antiferromagnetism is only weakly supported by virtual spin flips).

An important feature of the charge gap's evolution is that it does not close at the center of the reduced (mod $\boldsymbol{Q}$) Brillouin zone. As the system is driven through the

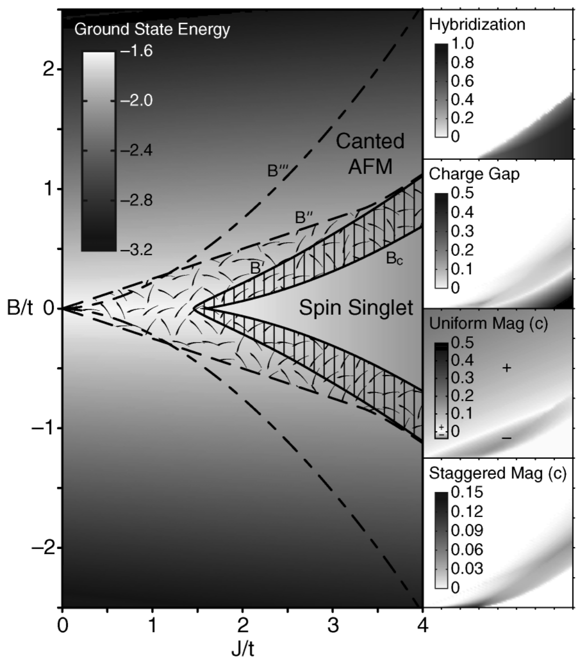

FIG. 1. $T = 0$ mean field, square lattice. (Left) B_{c} is a second-order transition; B', B'', and B''' are crossovers. The singlet phase has hybridization order only. Antiferromagnetic and hybridization order coexist in the striped region. The stippling indicates that the electron moments are directed to opposite the B field. For $|B| \gtrsim B'''$, the charge gap is exponentially small. Along the line $J < J_{\mathrm{c}}$, $B = 0$, the system is Néel ordered (uncanted). (Right) $\langle f^\dagger c \rangle$, Δ_{c}, $\langle \frac{1}{2} c_i^\dagger \sigma^3 c_i \rangle$, and $\langle (-1)^i \frac{1}{2} c_i^\dagger \sigma^1 c_i \rangle$ in the upper half of the phase diagram.

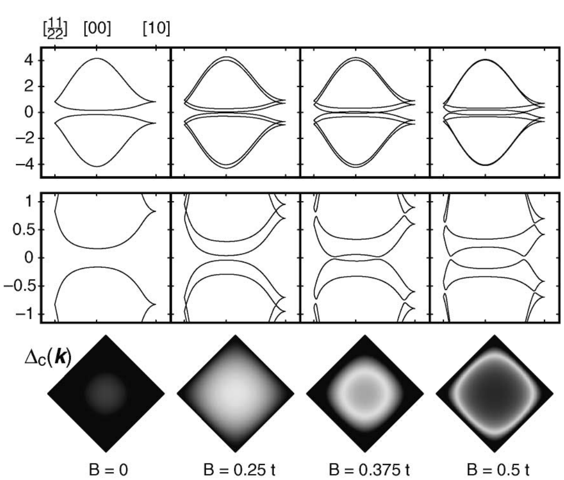

FIG. 2. $J/t = 3$, $B_{\mathrm{c}}/t \doteq 0.323$. (Top row) Mean field band structure, folded into the reduced Brillouin zone, as a function of applied magnetic field. (Middle) Same, magnified to show the evolution of the band gap. (Bottom) The greyscale (white–black $\leftrightarrow$ 0–0.5t) indicates the wave-vector-dependent gap magnitude. For $|B| < B_{\mathrm{c}}$, $\Delta_{\mathrm{c}}(\boldsymbol{k})$ is a minimum at $\boldsymbol{k} = 0$, and, for $|B| > B_{\mathrm{c}}$, at an expanding ring of points.

antiferromagnetic phase ($B_c < |B| \lesssim B'''$), the gap migrates from $\boldsymbol{k} = 0$ out to the zone edge. A consequence is that the hybridization energy and not the Kondo energy determines the robustness of the insulating state. This leads to a separation of energy scales: the spin gap closes when $|B| \sim 2\Delta_K$, whereas the charge gap (nearly) closes when $|B| \sim \sqrt{2\Delta_K W}$.

Quantum Monte Carlo.—The partition function of the system can be written as

$$Z = \int d\eta d\bar{\eta} e^{\bar{\eta}\eta} \langle \eta | \prod_{k=1}^{L} \hat{P} \int \mathcal{D}\chi_k e^{-\epsilon \hat{H}[\chi_k]} \hat{P} | -\eta \rangle, \quad (4)$$

where k labels the slices of discretized imaginary time ($\epsilon = \beta/L$), the Grassman vector $\eta = (c_\uparrow\ c_\downarrow\ f_\uparrow\ f_\downarrow)$ holds the four fermionic species, and the operator $\hat{P}$ projects out states that violate the single occupancy requirement of the f electrons. $\hat{H}[\chi_k]$ is bilinear and related to the Hamiltonian by a Hubbard-Stratonovich decomposition of the Kondo interaction in the hybridization channel.

Replacing $e^{-\epsilon \hat{H}[\chi_k]}$ by its coherent state representation puts a set of Grassman states at each time slice k. The matrix elements $\langle \eta_k | \hat{P} | \eta_{k+1} \rangle$ can be handled by introducing a U(1) gauge field $z_{k,k+1}$ living on the temporal links. Integrating out the Grassman fields gives $Z = \int \mathcal{D}\chi \times \mathcal{D}z e^{-S[\chi,z]}$, where $S = \sum_{i,k} |\chi_{i,k}|^2 - \mathrm{Tr} \ln M[\chi, z]$ is the action of a lattice gauge theory in $d + 1$ dimensions. By exploiting the particle-hole symmetry of the Hamiltonian and the bipartite nature of the lattice, it is possible to transform to a gauge in which M is positive definite. Specifically, under $c_{i\uparrow} \to c_{i1}$, $c_{i\downarrow} \to (-1)^i \bar{c}_{i2}$, $f_{i\uparrow} \to f_{i1}$, $f_{i\downarrow} \to (-1)^{i+1} \bar{f}_{i2}$, the gauge theory acquires a block diagonal form, $M = \mathrm{diag}(M_1, M_2)$ with $M_2 = M_1^\dagger$, so that $\det M = |\det M_1|^2$. Since the total magnetic moment transforms as $\sum_i (\bar{c}_i \sigma^3 c_i + \bar{f}_i \sigma^3 f_i) \to \sum_i \sum_{s=1,2} (\bar{c}_{is} c_{is} + \bar{f}_{is} f_{is})$, the positivity of M is preserved even for $B \neq 0$.

A general n-particle correlation function of the form $Z^{-1} \int \mathcal{D}\chi \mathcal{D}z M^{-1}_{i_1 i_1'; \tau_1 \tau_1'} \cdots M^{-1}_{i_n i_n'; \tau_n \tau_n'} e^{-S[\chi,z]}$ is evaluated via stochastic sampling [7] by interpreting $\mathcal{P}[\chi, z] = Z^{-1} e^{-S[\chi,z]}$ as a probability weight. (Since $\det M > 0$, there is no fermion sign problem.) This amounts to binning and tabulating $M^{-1}_{ii';\tau\tau'}$ for a large series of independent field configurations. Updates are effected by a more sophisticated version of the algorithm introduced by Blankenbecler, Scalapino, and Sugar [8]. Our method is related to that of Capponi and Assaad, who have carried out QMC for the KLM in zero field [5]. The reliability of our code is verified by comparison with their results: e.g., our computed critical coupling, $J_c/t = 1.47 \pm 0.08$, is consistent with their value of 1.45 ± 0.05.

The one-particle electron Green's function $G(\boldsymbol{k}, \tau) = \langle T[c_{\boldsymbol{k}}(0) c^\dagger_{\boldsymbol{k}}(\tau)] \rangle$ corresponds to $\int \mathcal{D}\chi \mathcal{D}z M^{-1}_{\boldsymbol{k};0\tau} \mathcal{P}[\chi, z]$. Written in terms of its spectral function $A(\boldsymbol{k}, \omega)$, the Green's function has the form of a linear functional $G(\boldsymbol{k}, \tau) = \int d\omega K(\tau, \omega) A(\boldsymbol{k}, \omega) = \mathbf{K}[A(\boldsymbol{k}, \omega)]$ with kernel $K(\tau, \omega) = e^{-\omega\tau}/(e^{-\beta\omega} + 1)$. To extract $A(\boldsymbol{k}, \omega)$, we perform a functional inversion $A(\boldsymbol{k}, \omega) = \mathbf{K}^{-1}[G(\boldsymbol{k}, \tau)]$. Since the input data are noisy and incomplete, however, the inversion problem is ill posed and must be systematically regularized. The most widely used procedure is the method of maximum entropy [9]. We employ a generalization of maximum entropy, which, rather than selecting a single most probable solution, averages (in the spirit of Ref. [10]) over a series of likely candidates. We believe that this method does a better job of extracting fine spectral features from data of low quality (i.e., having poor statistics).

Figure 3 shows the zero-field spectrum in the singlet phase ($J > J_c$). Note that the spectral peaks trace out two bands separated by a small gap at the chemical potential. The lower and upper bands exhibit (heavy fermion) regions of low spectral weight and nearly flat dispersion in the vicinity of $\boldsymbol{k} = (\pi, \pi)$ and $\boldsymbol{k} = 0$, respectively.

QMC results confirm that the KLM + Z system is described well by its mean field theory. Several signature features are observed in the simulations: a robust singlet phase ($J > J_c$, $|B| < B_c$), electronic moments directed against the field ($B_c < |B| < B''$), transverse staggered magnetic order ($B_c < |B| \lesssim B'''$), and a high-field ($|B| \sim B'''$) collapse of the charge gap near the reduced zone edge.

The inset of Fig. 4 depicts the phase boundary between the singlet and canted antiferromagnetic phases; it also marks where $\langle \frac{1}{2} c_i^\dagger \sigma^3 c_i \rangle$ changes sign. The main plot shows in six panels the spectral function of a spin up

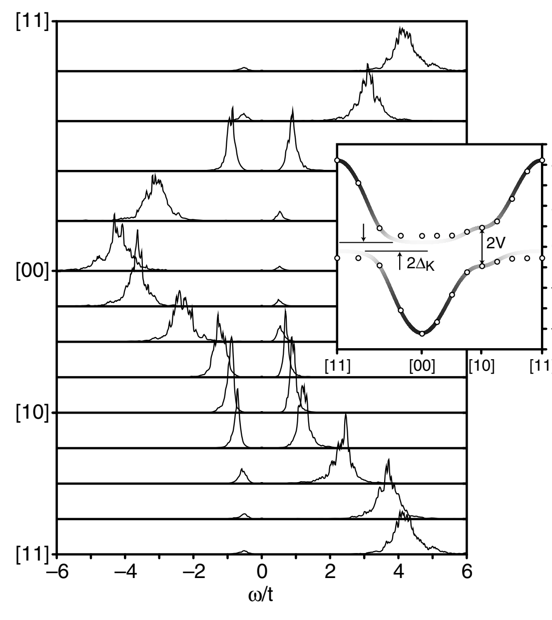

FIG. 3. Analytically continued data from the one-particle electron Green's function for $J/t = 1.7$, $\beta t = 14$ on an 8×8 lattice. Spectral functions $A(\boldsymbol{k}, \omega)$ are plotted for wave vectors along high-symmetry lines in the Brillouin zone. (Inset) the peak locations (open circles) are superimposed on the mean field band structure [Eq. (3)] with V chosen to fit the band splitting at $\boldsymbol{k} = (\pi, 0)$. The grey scale indicates the spectral weight (white–black ↔ 0–1).

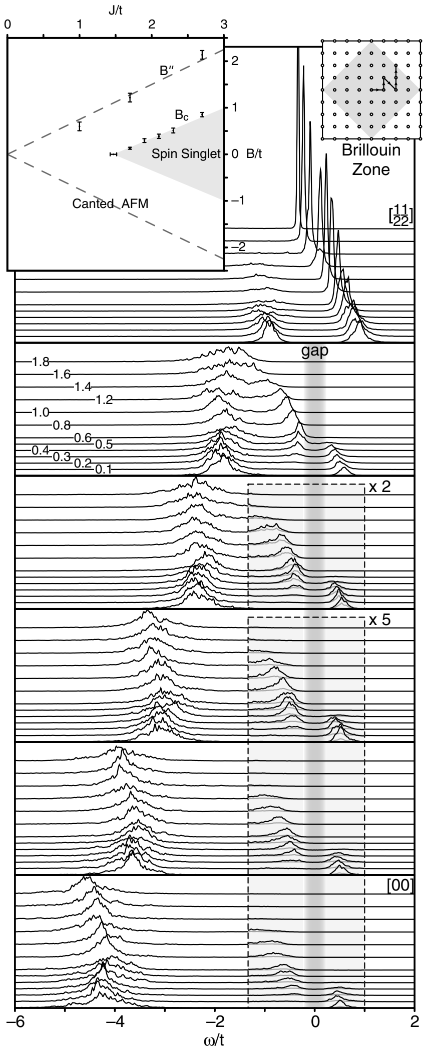

FIG. 4. $J/t = 1.7$, $\beta t = 14$, 8×8 lattice. Spectral functions $A_\uparrow(\boldsymbol{k}, \omega)$ are plotted over a range of field values ($0 \leq B/t \leq 1.8$ offset) for a series of wave vectors (identified in the top right inset). Smaller peaks have been scaled by the indicated magnification factor. Note that, instead of shifting smoothly through zero in a magnetic field, the spectral weight jumps across the gap, except for $\boldsymbol{k}$ on the reduced zone boundary. (Top left inset) A partial phase diagram. Electron moments are directed against the field between B_c and B''.

electron evaluated at a series of wave vectors snaking through the Brillouin zone from $\boldsymbol{k} = 0$ to $\boldsymbol{k} = (\pi/2, \pi/2)$; the panels are arranged (from bottom to top) in order of increasing distance from the zone center.

As per Eq. (3), the spectra exhibit a double peak structure and drift leftward (lowering energy) as B increases from zero. For small $\boldsymbol{k}$, there is a primary peak near the noninteracting particle energy $\omega = \varepsilon_{\boldsymbol{k}}$ and a secondary peak near $\omega = \Delta_K$. The leftward drift of the secondary peak is interrupted by the growth of antiferromagnetic correlations that protect the gap. *The spectral weight rearranges by hopping over the forbidden region.* There is no weight at the chemical potential, so the system remains insulating even when $|B| = 2\Delta_K$.

At $\boldsymbol{k} = (\pi/2, \pi/2)$, there are two equally weighted peaks at $\pm V$. As B is ramped up, spectral weight from the lower peak is transferred to the upper, unoccupied peak (this accounts for $\langle \frac{1}{2} c^\dagger \sigma^3 c \rangle < 0$), which grows increasingly sharper as it drifts leftward and crosses the chemical potential (fixed at $\mu = 0$ by particle-hole symmetry). To within the numerical resolution of the simulation, the antiferromagnetic correlations vanish; the spectral weight of the lower peak is exhausted and $A(\boldsymbol{k}, \omega) \to \delta(\omega - B/2)$, its free electron value.

In summary, we have investigated the effect of an applied magnetic field on the Kondo insulator ground state, using mean field calculations (in the thermodynamic limit) and QMC simulations (on small lattices) to characterize the phases of the KLM + Z. From these numerical results, a consistent picture emerges: (i) In the $J > J_c$ local singlet phase, the hybridized bands respond to the applied field by shifting with respect to one another and reducing the charge gap. (ii) For $|B| \sim 2\Delta_K$, the spin gap closes and the local singlet phase gives way to an antiferromagnetic phase in which the local spins cant *with* and the electron moments cant *against* the applied field. The hybridization-supported charge gap, which had nearly closed, reinflates, driven now by the magnetic order. (iii) At larger fields, there is a crossover at which the electron moments begin to cant with the field. (iv) For $|B| \gtrsim \sqrt{2\Delta_K W}$, the antiferromagnetism and charge gap are exponentially suppressed. The persistence of antiferromagnetic order, however, is an artifact of the perfectly nested Fermi surface. In a less idealized system, we expect the large-field regime to be a true metallic phase: the conduction electrons decouple from the quenched local spins and propagate freely.

This work was partially supported by the National Computational Science Alliance under Grant No. DMR020009 and by the Department of Energy under Grant No. DE-FG02-03ER46076. Computations were performed on the SGI Origin 2000 and IA-64 Linux Cluster. The authors thank T. M. Rice and Igor Milat for helpful discussions.

*Electronic addresses: ksdb@mit.edu

[1] P. Coleman, Phys. Rev. B **35**, 5072 (1987).
[2] S. Doniach, Physica (Amsterdam) **91B**, 231 (1977).
[3] M. Jaime *et al.*, Nature (London) **405**, 160 (2000).
[4] G. S. Boebinger *et al.*, Physica (Amsterdam) **211B**, 227 (1995).
[5] S. Capponi and F. F. Assaad, Phys. Rev. B **63**, 155114 (2001).
[6] G.-M. Zhang and L. Yu, Phys. Rev. B **62**, 76 (2000).
[7] N. Metropolis *et al.*, J. Chem. Phys. **21**, 1087 (1953).
[8] R. Blankenbecler, D. J. Scalapino, and R. L. Sugar, Phys. Rev. D **24**, 2278 (1981).
[9] M. Jarrell and J. E. Gubernatis, Phys. Rep. **269**, 133 (1996).
[10] A. W. Sandvik, Phys. Rev. B **57**, 10 287 (1998).